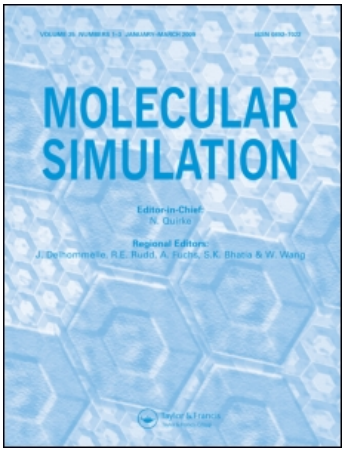

Molecular Simulation

Publication details, including instructions for authors and subscription information:
http://www.informaworld.com/smpp/title~content=t713644482

Predicting the Mechanical and Electrical Properties of Nanocomposites Formed from Polymer Blends and Nanorods

Gavin A. Buxton[a]; Anna C. Balazs[a]
[a] Department of Chemical and Petroleum Engineering, University of Pittsburgh, Pittsburgh, PA, USA

To cite this Article Buxton, Gavin A. and Balazs, Anna C.(2004) 'Predicting the Mechanical and Electrical Properties of Nanocomposites Formed from Polymer Blends and Nanorods', Molecular Simulation, 30: 4, 249 — 257
To link to this Article: DOI: 10.1080/08927020310001659142
URL: http://dx.doi.org/10.1080/08927020310001659142

Molecular Simulation, VOL. 30 (4), 15 April 2004, pp. 249–257

Taylor & Francis
Taylor & Francis Group

Predicting the Mechanical and Electrical Properties of Nanocomposites Formed from Polymer Blends and Nanorods

GAVIN A. BUXTON and ANNA C. BALAZS*

Department of Chemical and Petroleum Engineering, University of Pittsburgh, Pittsburgh, PA 15261, USA

(Received July 2003; In final form November 2003)

By integrating different simulation techniques, we investigate the self-assembly and macroscopic properties of nanocomposites composed of nanoscale rods and a binary polymer blend. In particular, we combine a Cahn–Hilliard (CH) theory for binary mixtures and a Brownian dynamics (BD) for nanorods to create a hybrid model that allows us to determine the structural evolution of the nanocomposite. The incorporation of the nanorods into the minority phase of the phase-separating blend yields a bicontinuous morphology, where the nanorods form a percolating network within the continuous minority phase. This morphology serves as the input to a lattice spring model (LSM), which is used to determine the mechanical properties, and a finite difference model (FDM), which is used to calculate the electrical conductance of the material. We find that in this doubly percolating system, the reinforcement efficiency of the nanorods and the electrical conductivity of the material are significantly increased relative to the behavior in composites where the nanorods are randomly dispersed in a homogeneous matrix. The integration of these various techniques allow us to predict the complex nanorod/polymer morphologies as a function of the constituents' characteristics, determine the mechanical and electrical, behavior of the resultant material and consequently relate the nanoscopic structure of the mixture to the macroscopic properties of the composite.

Keywords: Cahn–Hilliard theory; Nanocomposites; Brownian dynamics; Polymer blends

INTRODUCTION

Various properties of polymeric materials can be substantially improved through the inclusion of nanoscale solid particles, or "fillers". For example, the mechanical performance of a soft polymer can be significantly enhanced through the addition of such hard fillers. In this context, nanoscopic particles are particularly advantageous because they give rise to relatively large interfacial regions between the polymer and particles within the composite. These large interfacial regions facilitate stress transfer between the soft matrix and the stiffer inclusions; such efficient stress transfer plays a crucial role in dictating the mechanical performance of the material. The beneficial attributes of the particles are further improved when these fillers percolate to form a continuous network throughout the material. In particular, the percolating structure can result in dramatic increases in the reinforcement efficiency of the fillers (by providing a continuous backbone of stiff reinforcing material) [1]. If the particles are semiconductors or metals, the percolation of the particles can also significantly increase the electrical conductivity of the system (by creating a direct path for electrical transport across the material) [2].

Nanoscale rods are becoming increasingly important additives in the fabrication of polymer composites [3,4]. The high aspect ratio (and high surface area) of nanorods results in polymer nanocomposites that can possess superior mechanical properties relative to polymers reinforced with an equivalent volume fraction of spherical inclusions [5]. Recently, Huyne *et al.* [3] blended inorganic nanorods and polymers to fabricate solar cells that possess greater efficiencies than conventional organic photovoltaic cells. In this application, nanorods were preferable, in part, because they naturally provide a direct pathway for charge transport. Peng *et al.* [6] showed that immersing nanorods into a binary phase-separating blend can drive the rods to form

*Corresponding author. E-mail: balazs@pitt.edu

ISSN 0892-7022 print/ISSN 1029-0435 online © 2004 Taylor & Francis Ltd
DOI: 10.1080/08927020310001659142

percolating networks at relatively low volume fractions. These extensive networks can potentially improve both the mechanical and electrical properties of the polymer/nanorod mixtures. To facilitate the design of such high-performance materials, it is useful to correlate the microstructure of the filler network and the macroscopic properties of the polymeric composite. In order to establish these correlations, in this paper we integrate different computational techniques to simulate both the morphological evolution of a binary blend that contains nanorods and the mechanical and electrical properties of the resultant nanocomposite.

To determine the morphology of a mixture of binary phase-separating fluids and nanorods, we use a hybrid method [1,6–11] that combines a Cahn–Hilliard (CH) model for the binary mixture and a Brownian dynamics (BD) for the particles. Through this CH–BD method, we can determine how the phase separation of the fluid affects the dispersion of the particles and how the fluid–particle interactions, in turn, affect the evolution of the binary mixture. Furthermore, we can include interactions between the particles and investigate how these interactions influence the morphology of this system.

The morphologies obtained from our CH–BD simulations serve as the input to either a micromechanical simulation or an electrical simulation. Here, we use a lattice spring model (LSM) to capture the micromechanics of the complex heterogeneous structures obtained via the CH–BD method. The lattice in the LSM consists of a network of nearest and next-nearest neighbor interactions, which are harmonic in nature. These harmonic interactions, or "springs", result in linear forces between lattice sites (nodes). Thus, the LSM can be considered as a network of interconnecting one-dimensional springs. The nature of the interactions between the nodes define the class of LSMs. In this study, we employ the Born LSM [12,13]. The Born LSM includes central force harmonic interactions (parallel to the springs) and a noncentral two-body harmonic potential (perpendicular to the springs), which limits the rotational freedom of the springs. This model possesses a Poisson's ratio of some variability (through the variation of the noncentral force constant), but the model is not rotationally invariant. The Kirkwood–Keating LSM introduces more complicated three-body interactions, which energetically penalize the angular variations between bonds, and is therefore rotationally invariant [14–16]. In these studies, however, we assume that the rotations are small and we therefore adopt the Born LSM. LSMs have been used to elucidate the deformation of two-dimensional particulate systems [17–19], including the deformation of rod-polymer composites [20,21]. Through these models, one can capture not only the local deformation fields but also, the global Young's modulus of heterogeneous materials.

In order to investigate the electrical conductivity of the heterogeneous polymer/nanorod composites, we discretize Laplace's equation for a static current distribution onto a square lattice [22]. This is equivalent to solving Ohm's law (voltage is linearly related to current) and Kirchoff's law of current conservation (total current flowing into any point is zero) for a network of resistors [23]. The resistor network model offers an expedient method for discretizing the electrical behavior of a continuous medium, while allowing for the heterogeneous nature of this material.

It is worth noting that a significant technological push in the formulation of nanocomposites is the creation of multifunctional materials, which exhibit a broad spectrum of desired properties [24]. In this context, it becomes important to develop a suite of computational tools that can be used to predict a range of properties (e.g. mechanical, electrical, thermal) for a specific nanocomposite formulation. In this manner, the designer can correlate the characteristics of the mixture to the performance of the material. By carrying out the calculations in an iterative manner, one can also carry out a trade-off analysis, determining how to optimize the mixture to meet a variety of desired specifications. The calculations described here present a step in providing computational methods for relating the microstructure of nanocomposites and the mechanical and electrical properties of the system. Here, we vary the volume fraction of the nanorods and the nature of the matrix material (binary mixture versus homogeneous medium). Further refinements in the behavior of the material could be achieved by varying the composition of the blend or the length of the rods. We leave these studies for future work.

In the next section, we detail the computational methodologies employed in this study. The results and relevant discussions are presented in the third section, while conclusions are drawn in the final section.

METHODOLOGY

In this section, we describe the computational techniques that we use to describe the evolution of a mixture containing nanoscale rods and a binary, phase-separating blend, and the mechanical and electrical properties of the resultant solid composites.

Morphological

In order to determine the morphologies of polymer nanocomposites, we employ a hybrid approach that describes the phase separation of the *AB* polymer blend through a CH model and the dispersion of

the nanoparticles through BD. We begin by describing the CH component of the model. We define the scalar order parameter Ψ as the difference in the local densities of the A and B components, i.e. $\Psi = \rho_A - \rho_B$, where ρ_A and ρ_B are the respective local densities of A and B. The value $\Psi = 1(-1)$ corresponds to the equilibrium order parameter of the A-rich (B-rich) phase. The CH theory [25,26] captures the evolution of phase-separating AB binary mixtures through the following kinetic equation

$$\frac{\partial \Psi}{\partial t} = M\nabla^2 \frac{\partial F}{\partial \Psi} + \xi \tag{1}$$

where M is the kinetic coefficient (mobility) of the order parameter. The conserved zero-mean white noise, ξ, is set to zero in these simulations. We take the free energy functional, F, to be $F = F_b + F_{cpl} + F_{rr}$, where F_b describes the local and gradient energy contributions and is given by

$$F_b = \int -A \ \ln[\cosh(\Psi)] + \frac{1}{2}\Psi^2 + \frac{D}{2}(\nabla\Psi)^2 \partial \mathbf{r} \tag{2}$$

where A and D are material specific parameters. Here, we set $A = 1.3$ and $D = 0.5$.

The second term of the free energy, F_{cpl}, describes the interactions between the nanorods and the polymers. We assume that the rods are coated with a layer of the A component. Due to this coating, the free energy of the system is lowered when the rods are preferentially localized in the A phase of the blend. Mathematically, this interaction is described in the following manner:

$$F_{cpl} = \int \sum_i \int V(\mathbf{r} - \mathbf{s}_i) \left(\Psi(\mathbf{r}) - \Psi_w\right)^2 \partial \mathbf{s}_i \, \partial \mathbf{r} \tag{3}$$

where $\mathbf{s}_i$ represents a point on the surface of the ith nanorod, and $\Psi(\mathbf{r})$ is the value of the order parameter at point $\mathbf{r}$. By setting $\Psi_w = 1$, we model the preferential wetting interaction between the rods and the A phase. The function $V()$ describes the short range interaction between the surface of the rod and the blend and is given by

$$V(\mathbf{r} - \mathbf{s}_i) = V_0 \exp\left(-\frac{|\mathbf{r} - \mathbf{s}_i|}{r_0}\right) \tag{4}$$

where V_0 is a constant and r_0 dictates the range of the interaction.

The rod–rod interaction, F_{rr}, is taken to be repulsive and is dependent upon the distance and angle between two rods

$$F_{rr} = \begin{cases} \chi \sum_i \sum_j \left(L - |\mathbf{r}_i - \mathbf{r}_j|\right)^2 \left[\frac{4}{3} - \cos^2(\theta_i - \theta_j)\right] & \text{for} \quad |\mathbf{r}_i - \mathbf{r}_j| < L \\ 0 & \text{for} \quad |\mathbf{r}_i - \mathbf{r}_j| \geq L \end{cases} \tag{5}$$

where the constant χ characterizes the strength of the interaction, L is the rod length, and $\mathbf{r}_i$ and θ_i are the respective position of the ith rod and its angle relative to a fixed direction. One way to simultaneously achieve the preferential wetting interaction described above and the rod–rod repulsion is to anchor A chains onto the surface of the rods. The compatibility between the anchored chains and the chemically identical A phase will yield the desired wetting behavior and the steric interactions between the grafted chains will lead to an effective repulsion between the rods. In the absence of the binary blend, F_{rr} leads to an isotropic-nematic ordering for the pure rod system [6].

These equations are solved in a computationally efficient manner through the employment of a cell dynamics scheme (CDS) [27,28]. The use of a CDS (rather than a conventional discretization of Eqs. (1) and (2)) significantly reduces the computational expense of the simulations.

The rigid rods are described as discreet entities [6], each of which has a center-of-mass position $\mathbf{r}_i$ and an orientation angle θ_i, measured from a fixed direction. The position $\mathbf{r}_i$ and angle, θ_i of the ith rod is updated using the following Langevin equations

$$\frac{\partial \mathbf{r}_i}{\partial t} = -M_r \frac{\partial F}{\partial \mathbf{r}_i} + \xi_r \qquad \frac{\partial \theta_i}{\partial t} = -M_\theta \frac{\partial F}{\partial \theta_i} + \xi_\theta \tag{6}$$

where M_r and M_θ are the respective translational and rotational mobility constants, and ξ_r and ξ_θ represent thermal fluctuations that satisfy the fluctuation-dissipation relations. Here, we set $M_r = 1$ and $M_\theta = 1$. Equation (6) is discretized and solved numerically.

The above equations describe how an immiscible polymer blend evolves in the presence of nanoscale rods, and how nanoscale rods are affected by the polymer blend. Now, we describe how the mechanical properties of these composites can be determined.

Mechanical

In order to simulate the micromechanics of the highly heterogeneous nanorod/polymer mixture considered here, we utilize the LSM. The Born LSM employed in this study consists of a network of nearest and next-nearest interactions, which can be locally varied to account for local variations in

the stiffness of heterogeneous systems. The interactions are harmonic in nature and the energy associated with the ith node is given by

$$F_i = \frac{1}{2}\sum_j (\mathbf{u}_i - \mathbf{u}_j)\cdot\mathbf{M}_{ij}\cdot(\mathbf{u}_i - \mathbf{u}_j) \tag{7}$$

where $\mathbf{u}_i$ is the displacement of the ith node from its original position, $\mathbf{M}_{ij}$ is a symmetric matrix of constants, which describe the central and non-central interactions between nodes i and j, and the summation is over all neighboring nodes. Through the appropriate choice of parameters, this Born spring model can be shown to recover linear elasticity theory [13], resulting in the following expressions (in two-dimensions) for the Young's modulus, E, and Poisson's ratio, μ.

$$E = \frac{4K(K+C)}{3K+C} \quad \mu = -\frac{K-C}{C+3K} \tag{8}$$

where K and C are the central and non-central force constants, respectively.

The harmonic form of Eq. (7) results in linear forces between neighboring nodes. The constraint that all these linear forces must balance at each node at equilibrium results in a set of linear equations, which can be solved using a conjugate gradient solver [13]. For a system in equilibrium, we can take the average displacement of boundary nodes in the tensile direction and calculate the global Young's modulus (applied stress divided by strain), thereby obtaining a global macroscopic description of the composite derived from the local constituent properties.

The local force constants are specified at nodal points at the beginning of the simulation, and the value of these constants depends on whether or not a node is within the polymer blend or a stiff rod. A force constant between nodes i and j, K_{ij}, is then simply taken to be the average of the force constants at nodes i and j, i.e. $K_{ij} = K_i/2 + K_j/2$. (Here, we assume $C = 0$, and thereby fix the Poisson's ratio at 0.33.) In order to capture the local deformation of the inclusions, we enlarge the lattice size by a factor of sixteen and, thereby, minimize discretization effects. For example, a CH–BD simulation consisting of 256×256 nodes would result in a LSM simulation of 1024×1024 nodes. In this manner, the morphologies generated using the combined CH–BD approach are directly fed into the LSM and the mechanical properties of a composite are directly related to the polymer and rod characteristics.

Electrical Model

In addition to investigating the mechanical properties of polymer blends reinforced with nanorods, we elucidate the electrical behavior of this nanocomposite. The condition for the conservation of current, $\mathbf{J}$, in a closed electrical circuit is $\nabla\cdot\mathbf{J} = 0$. Ohm's law relates the current to the electric field, $\mathbf{J} = G\mathbf{E}$, where G is the conductivity. Thus, we can write

$$\nabla\cdot(G\mathbf{E}) = 0 \tag{9}$$

Since the electric field is the gradient of the electric potential, Φ, we obtain the following equation for an inhomogeneous system

$$\nabla\cdot(G\nabla\Phi) = 0 \tag{10}$$

Taking a finite difference approximation results in the following discrete equation

$$\sum_j G_{ij}[\Phi_j - \Phi_i] = 0 \tag{11}$$

where the summation is over the neighboring nodes on a square lattice, G_{ij} is the conductance between nodes i and j, and Φ_i is the potential at node i. Equation (11) is simply a combination of Ohm's law and Kirchoff's law of current conservation for a square network [23]. The above system of equations are solved with constant voltages being applied to the boundaries of the system in the x-direction.

Just as in the micromechanical studies, the morphologies generated from the CH–BD simulations serve as input to the electrical model. The conductivities are assigned to the lattice nodes at the beginning of the simulation; the specific value at a node depends upon its location, i.e. if it is situated in a polymer domain or a rod. In order to assign a conductivity between two neighboring sites, we take the sites to be in series. In other words, the conductivity between nodes i and j is given by $G_{ij} = (1/2G_i + 1/2G_j)^{-1}$. The rods are assigned a higher conductance than the polymers. In particular, the rods are ten times more conductive than the polymer matrix. In these conductivity studies, we also enlarge the size of the simulation box by a factor of sixteen. With the voltage being applied at the system boundaries, we obtain the current flow through this heterogeneous system. In this manner, we obtain the global conductance as a function of the composition of the nanocomposite.

RESULTS AND DISCUSSIONS

We first present the morphology results from the CH–BD simulations. We vary the volume fraction of the nanorods, which are incorporated into a 30:70 AB polymer blend. As noted above, the rods are preferentially wet by the minority A phase. These morphological studies are very similar to those carried out by Peng *et al.* [6]. Here, however, our aim

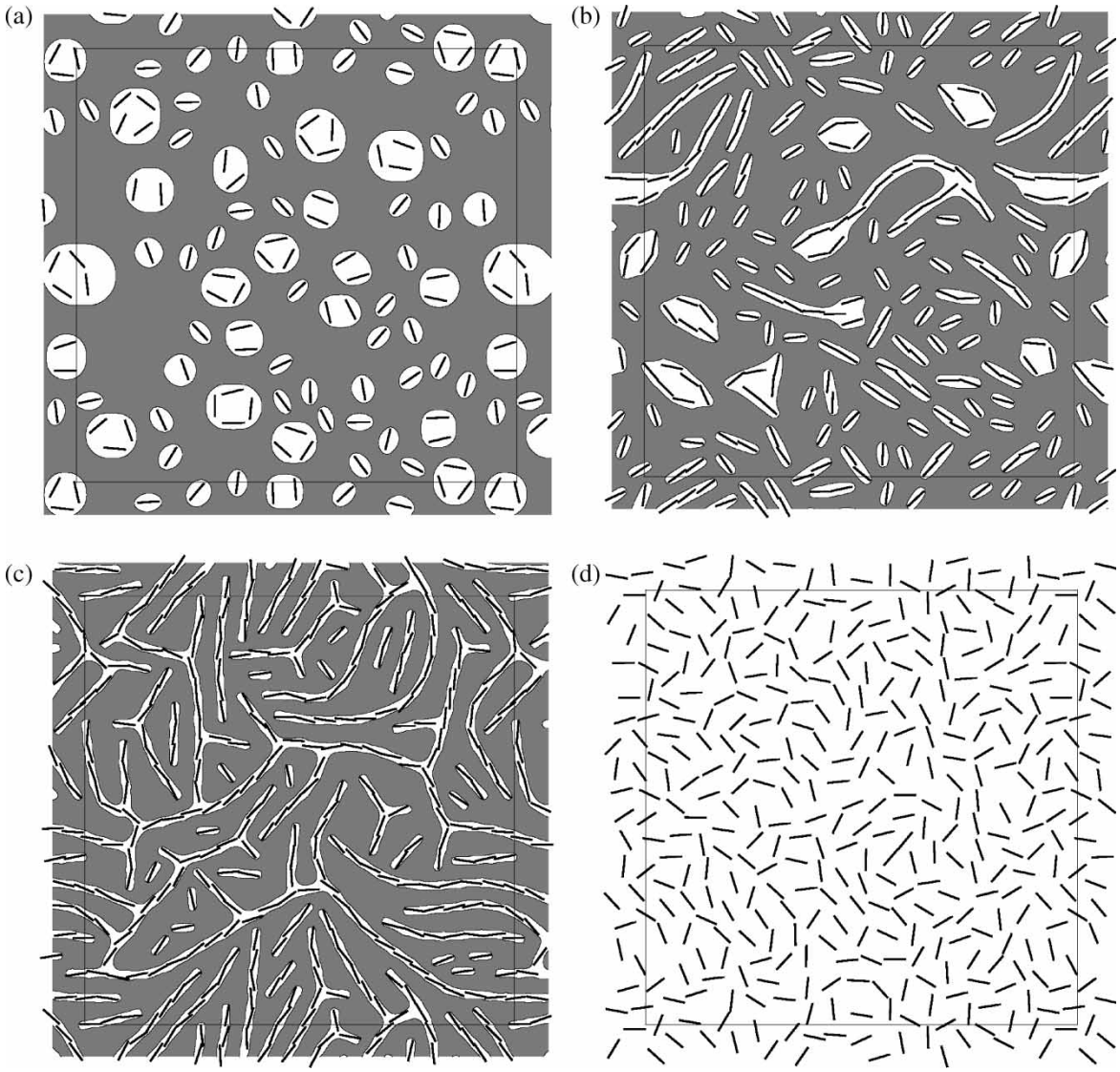

FIGURE 1 Morphology of nanorod/polymer blend system for (a) 2%, (b) 4% and (c) 6% volume fraction of nanorods. White regions are the minority phase *A*, gray regions are the majority phase *B*, a contour line separates them at $\Psi(\mathbf{r}) = 0$ and the rods are shown as black rectangles. (d) The morphology for a system of 6% volume fraction of nanorods within a homogeneous matrix.

is to extend these studies by relating the microstructure of the mixture to the macroscopic properties of the nanocomposite. With this aim in mind, we contrast the local deformation fields and the global Young's modulus for two separate nanorod/polymer mixtures. In the first case, the rods are introduced into the binary, phase-separating blend. In the second case, the rods are dispersed in a homogeneous matrix (e.g. a homopolymer); here, we neglect the CH equation and simply numerically solve the equation of motion [Eq. (6)] for the rods. We find that the localization of the nanorods into the minority phase of the phase-separating blend leads to substantial improvements in the reinforcement efficiency of the rods. Finally, we compare the local current densities for the above two cases and find a relative increase in the electrical conductivity in the system where the nanorods are selectively incorporated into the minority phase of the blend.

Morphology: Formation of Supramolecular Networks

The distribution of nanoscale inclusions within a polymer matrix can yield an appreciable influence over the macroscopic properties of the nanocomposite. We first consider the effects of incorporating the nanoscale rods into the minority *A* phase of the 30:70 *AB* blend. In particular, we examine the effects of increasing the volume fraction of these rods on the microstructure of the complex mixture. The rods have a width *W* of one lattice site and a length *L* of 13 lattice sites. The size of the two-dimensional simulation box is 256×256 lattice sites. In Fig. 1(a)–(c), we present the respective

morphologies of nanocomposites that contain rod volume fractions of 2, 4 and 6%. The morphologies represent the system at the late stage of domain growth ($t = 600,000$). The minority A phase is shown as white domains and the majority B phase is shown as grey domains. A black contour line is drawn at $\Psi(\mathbf{r}) = 0$. The rods are shown as black rectangles. As a basis of comparison, Fig. 1(d) shows the structure of a 6% volume fraction of rods in a homogeneous matrix (in the absence of the phase-separating blend).

Figure 1(a) depicts the structure of the system that is loaded with a 2% volume fraction of rods. The rods are clearly located within the minority A phase. The A domains are dispersed throughout the system, with smaller domains containing a single rod and larger domains containing multiple rods. The shapes of the smaller domains are perturbed from circular to ellipsoidal by the presence of the rods. The larger domains appear less affected by the presence of these fillers.

The consequences of increasing the volume fraction of the rods from 2 to 4% can be seen in Fig. 1(b). Again the A domains are dispersed throughout the system but now, the domain shapes are appreciably different from those shown in Fig. 1(a). Smaller domains containing a single rod are still ellipsoidal but now, domains that contain more than one rod have a tendency to be elongated. The coupling between the wetting interactions and the rod–rod repulsion has led to the rods being aligned end-to-end within the A phase. Furthermore, the A phase has been stretched by the presence of the rods. This cooperative behavior leads to the formation of "string-like", reinforced A domains. Further increases in the volume fraction of rods enhances these effects.

Figure 1(c) shows the morphology for a system containing 6% volume fraction of rods. Increasing the volume fraction of rods has increased the elongation of the minority domains to the extent that they now interconnect and form continuous domains across the system. The rods are "corralled" into these elongated domains to such an extent that they percolate throughout these domains [6]. The percolation of these nanoscale inclusions and the continuous nature of the minority A phase results in a system that exhibits double percolation.

Within a homogeneous matrix, the 6% volume fraction of rods are uniformly dispersed in the system, as shown in Fig. 1(d). This volume fraction is below the critical value at which the rods display a nematic ordering [6] and the system is in the isotropic phase. This uniform distribution is in distinct contrast to the highly organized structure seen in Fig. 1(c); the electrical and mechanical benefits of having the nanorods distributed in this controlled manner are discussed below.

Mechanical Properties

Here, we assume that the rods are ten times stiffer than the polymeric matrix (both the A and B components are assumed to have the same stiffness) and investigate the effects of rod distribution on the local and global elasticity of the nanocomposite. In particular, we fix the volume fraction of rods at 6% and compare the local deformations in a system where the rods are corralled by a polymer blend into percolating pathways with a system where the rods are allowed to evolve in a homogeneous matrix. We also compare the global Young's modulus as a function of the rod volume fraction for these two distinct systems. In order to carry out these calculations, we apply a stress field at the LSM boundaries in the x-direction, thus defining the tensile direction.

The local relative normal stress field is defined as $(\sigma_{xx} - \sigma_0)/\sigma_0$ where σ_{ij} is the stress tensor and σ_0 is the normal stress field of an unreinforced polymer, i.e. a homogeneous material that does not contain rods. Figure 2 shows these stress fields for rods dispersed in a homogeneous matrix [Fig. 2(a)] and in a phase-separating blend [Fig. 2(b)]. Stress concentrations within the rods can be seen as lighter regions, corresponding to higher stresses. The darker regions correspond to lower stresses and can be seen

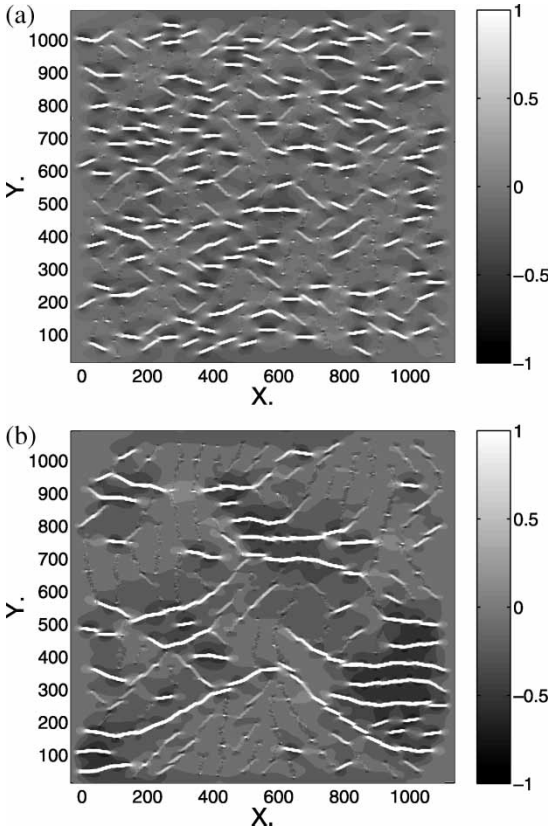

FIGURE 2 Normal stress field contours for (a) 6% nanorods in a homogeneous system and (b) 6% nanorods in a phase-separating system.

within the polymer matrix surrounding the rods. Rods oriented in the tensile direction (x-direction) have a greater effect on the stress field than rods oriented normal to x; in particular, rods oriented along x exhibit greater stress concentrations and cause lower stresses within the neighboring polymeric material. This can be seen in Fig. 2(b), which depicts the stress field for the phase-separating system. In regions where the local domains are aligned in the tensile direction, the rods are clearly visible as regions of high stress, whereas regions where the local domains are aligned normal to the tensile direction possess lower stress perturbations (at the ends of the rods). Because the stiff rods prohibit the matrix from deforming, the polymeric material that is confined between neighboring rods exhibits particularly low stress. In other words, there is efficient stress transfer from the softer polymer matrix to the stiffer rods.

The local relative normal strain field is defined as $(u_{xx} - u_0)/u_0$, where u_{ij} is the strain tensor and u_0 is the normal strain field of an unreinforced polymer. These strain fields are presented in Figure 3. The positions of the stiffer rods are apparent from the dark regions of lower strains. What is of most interest is the manner in which the matrix is prohibited from deforming. Figure 3(a) shows

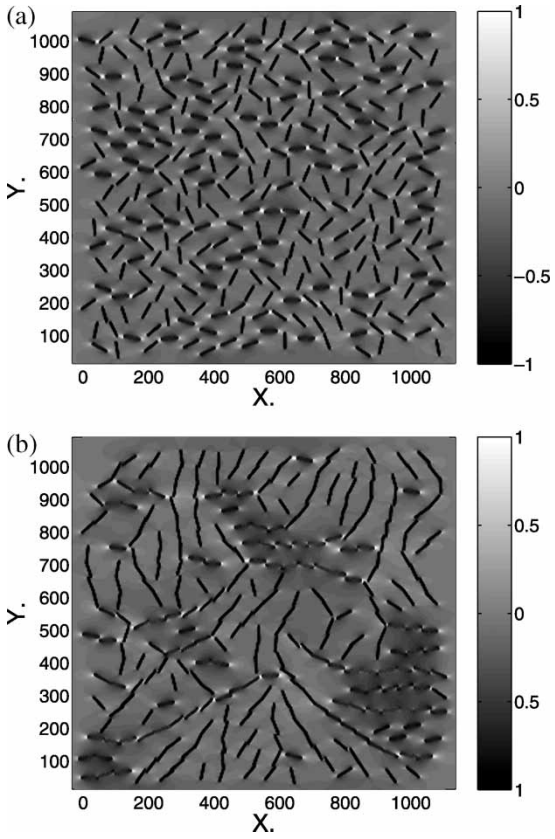

FIGURE 3 Normal strain field contours for (a) 6% nanorods in a homogeneous system and (b) 6% nanorods in a phase-separating system.

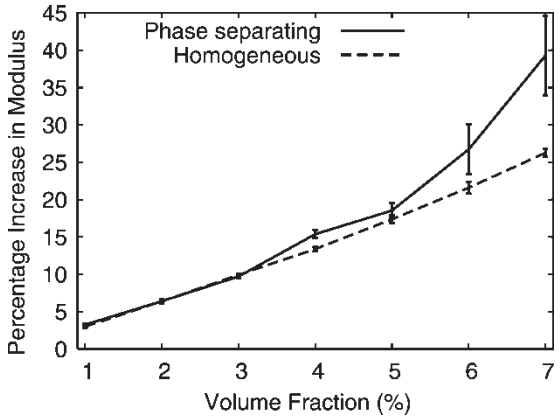

FIGURE 4 The percentage increase in Young's modulus as a function of nanorod volume fraction.

the local strains for a homogeneous system, where the rods are dispersed uniformly throughout the system. Rods aligned with the tensile direction induce strain concentrations within the polymer matrix at the edges of the rods and induce strain reductions at the sides of the rods. In contrast, rods that are aligned perpendicular to the tensile direction show little perturbation of the strain field around these inclusions. Figure 3(b) depicts the local strain field for a polymer blend with the rods confined within the minority phase. Regions where the domains are aligned with the tensile direction induce severe strain reductions as the local ordering of the polymer domains, and hence the corralled rods, prohibit the deformation of substantial regions of the polymer matrix. These regions of low strain have a macroscopic influence.

Figure 4 shows the percentage increase in the global Young's modulus relative to an unfilled (no rods), homogeneous material; the data is averaged over three independent realizations from the CH–BD calculations (at fixed volume fraction of rods) and the error bars represent the standard deviation. The solid line depicts data taken from the phase separating systems, while the dashed line represents data from the equivalent homogeneous systems. At lower volume fractions of rods, there is little difference between the two cases as the rods do not appreciably affect the polymer blend morphology and the polymer blend does not dramatically perturb the distribution of the rods. As the volume fraction of rods is increased, the polymer blend begins to form elongated domains, and when these domains are elongated in the tensile direction, significant improvements in the reinforcement efficiency of the rods ensue. This is especially the case at higher rod concentrations, where the system becomes doubly percolating and the rods form a continuous backbone of stiff material throughout the nanocomposite.

Next we consider the electrical benefits of loading nanorods into a phase separating system as opposed to a homogeneous system.

Electrical Properties

The conductivity of the rods is ten times greater than that for the polymer matrix. We assess how the rod distribution affects both the local electrical behavior and the global conductivity. Figure 5 shows the current density for systems containing 6% of the rods; in Fig. 5(a), the rods are dispersed in a homogeneous matrix and in Fig. 5(b), the rods are corralled into percolating pathways by the surrounding polymer blend. The current density at the ith node is defined as $I_i = \sum_j |G_{ij}[\Phi_j - \Phi_i]|$ and reflects the amount of current flowing through a given node. In Fig. 5(a), the current density is greater in the higher conductance rods and is especially high for rods that are oriented in the direction of potential gradient (x-direction). The current density within the rods is appreciably higher in Fig. 5(b) than in Fig. 5(a). The current flowing along the rods is greater when the rods are oriented in the same direction as the potential gradient. The percolating nanorods provide a direct pathway for electrical conductivity across the system. The effect that the percolating structure has on the global conductivity is considered below.

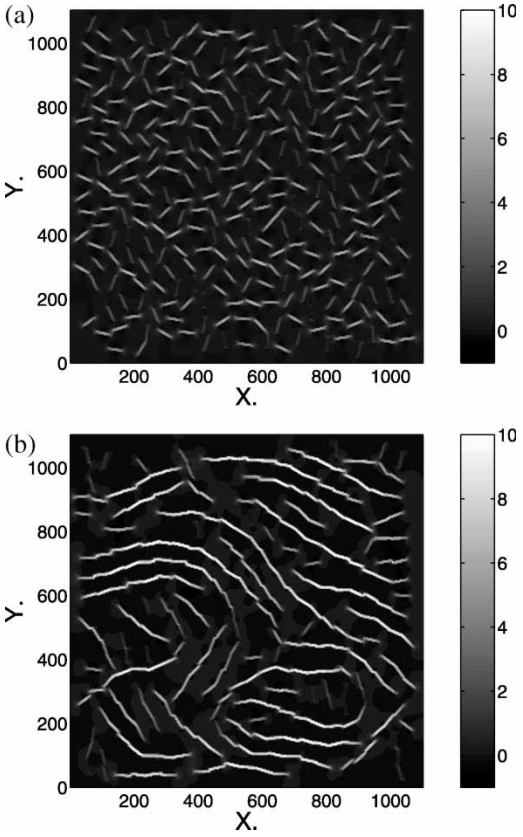

FIGURE 5 Current density contours for (a) 6% nanorods in a homogeneous system and (b) 6% nanorods in a phase-separating system.

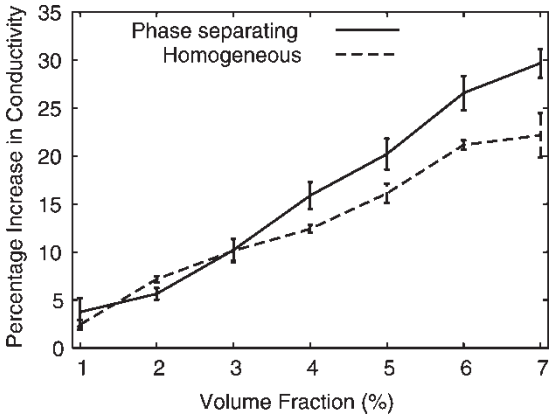

FIGURE 6 The percentage increase in conductivity as a function of nanorod volume fraction.

Figure 6 depicts the percentage increase in conductivity relative to an unfilled, homogeneous material and the data is averaged over three independent runs with the error bars reflecting the standard deviation. At lower volume fractions of rods, there is no benefit to incorporating them into a phase-separating polymer blend relative to adding them to a homogeneous polymer matrix. As the volume fraction of rods is increased, the elongated domains in the phase separating system corral the rods into pathways along which electrical transport is facilitated. As these domains span the system and the morphology becomes bicontinuous rather than dispersed, the increase in conductivity of the reinforced (rod-filled) polymer blend is roughly 8% greater than that of the reinforced homogeneous system. This demonstrates a clear advantage to incorporating the rods into the phase-separating system. It is anticipated that a greater disparity between the two systems would be observed if there were a more significant difference in the conductivities of the rods and polymers.

SUMMARY AND CONCLUSIONS

The selective inclusion of nanorods into the minority phase of a phase-separating polymer blend results in the emergence of complex networks of both nanorods and polymers [6]. The nanorods stretch and perturb the domains of the polymer blend, and the polymer blend confines and corrals the nanorods, producing elongated domains that are reinforced by these fillers. At a critical volume fraction of rods, the polymeric minority domains elongate to the extent that they coalesce with neighboring domains and form a continuous structure. The continuity of the minority domains and the percolation

of the nanorods within these domains results in a system that is doubly percolating.

We compare the mechanical behavior of such doubly percolating composites with materials where the rods are uniformly dispersed in a homogeneous matrix. In the former case, the nanorods form a continuous backbone of stiff, reinforcing material, which spans the system and results in a significantly stiffer nanocomposite. We also consider the electrical benefits of percolating nanorod networks for systems where the nanorods are more conductive than the polymer matrix. The nanorods provide a continuous path of high conductance across the composite, thus facilitating electrical transport.

The electrical and mechanical benefits of including nanorods is found to be direction dependent, with rods oriented in the tensile direction imparting greater stiffness and rods oriented with the potential difference gradient improving the conductivity. Controlling the direction in which these rods are orientated (e.g. through the application of an electric field during processing [29]) could lead to even greater improvements in macroscopic properties.

References

[1] Buxton, G.A. and Balazs, A.C. (2003) "Simulating the morphology and mechanical properties of filled diblock copolymers", *Phys. Rev. E* **67**, 031802.

[2] Gubbels, F., Jérôme, R., Teyssié, Ph., Vanlathem, E., Deltour, R., Calderone, A., Parenté, V. and Brédas, J.L. (1994) "Selective localization of carbon black in immiscible polymer blends: a useful tool to design electrical conductive composites", *Macromolecules* **27**, 1972–1974.

[3] Huynh, W.U., Dittmar, J.J. and Alivisatos, A.P. (2002) "Hybrid nanorod–polymer solar cells", *Science* **295**, 2425–2427.

[4] Mitchell, C.A., Bahr, J.L., Arepalli, S., Tour, J.M. and Krishnamoorti, R. (2002) "Dispersion of functionalized carbon nanotubes in polystyrene", *Macromolecules* **35**, 8825–8830.

[5] Buxton, G.A. and Balazs, A.C. (2002) "Lattice spring model of filled polymers and nanocomposites", *J. Chem. Phys.* **117**, 7649–7658.

[6] Peng, G., Qiu, F., Ginzburg, V.V., Jasnow, D. and Balazs, A.C. (2000) "Forming supramolecular networks from nanoscale rods in binary, phase-separating mixtures", *Science* **288**, 1802–1805.

[7] Ginzburg, V.V., Qiu, F. and Balazs, A.C. (2002) "Three-dimensional simulations of diblock copolymer/particle composites", *Polymer* **43**, 461–466.

[8] Ginzburg, V.V., Gibbons, C., Qiu, F., Peng, G. and Balazs, A.C. (2000) "Modeling the dynamic behavior of diblock copolymer/particle composites", *Macromolecules* **33**, 6140–6147.

[9] Balazs, A.C., Ginzburg, V.V., Qiu, F., Peng, G. and Jasnow, D. (2000) "Multi-scale model for binary mixtures containing nanoscopic particles", *J. Chem. Phys. B* **104**, 3411–3422.

[10] Ginzburg, V.V., Qiu, F., Paniconi, M., Peng, G., Jasnow, D. and Balazs, A.C. (1999) "Simulation of hard particles in a phase-separating binary mixture", *Phys. Rev. Lett.* **82**, 4026–4029.

[11] Ginzburg, V.V., Peng, G., Qiu, F., Jasnow, D. and Balazs, A.C. (1999) "Kinetic model of phase separation in binary mixtures with hard mobile impurities", *Phys. Rev. E* **60**, 4352–4359.

[12] Hassold, G.N. and Srolovitz, D.J. (1989) "Brittle fracture in materials with random defects", *Phys. Rev. B* **39**, 9273–9281.

[13] Buxton, G.A., Cleaver, D.J. and Care, C.M. (2001) "A lattice spring model of heterogeneous materials with plasticity", *Model. Simul. Mater. Sci. Eng.* **9**, 485–497.

[14] Schwartz, L.M., Feng, S., Thorpe, M.F. and Sen, P.N. (1985) "Behavior of depleted elastic networks: comparison of effective-medium and numerical calculations", *Phys. Rev. B* **32**, 4607–4617.

[15] Sahimi, M. and Arbabi, S. (1992) "Percolation and fracture in disordered solids and granular media: approach to a fixed point", *Phys. Rev. Lett.* **68**, 608–611.

[16] Monette, L. and Anderson, M.P. (1994) "Elastic and fracture properties of the two-dimensional triangular and square lattices", *Model. Simul. Mater. Sci. Eng.* **2**, 53–66.

[17] Monette, L., Anderson, M.P., Wagner, H.D. and Mueller, R.R. (1994) "The Young's modulus of silica beads/epoxy composites: experiments and simulations", *J. Appl. Phys.* **75**, 1442–1455.

[18] Ostoja-Starzewski, M., Sheng, P.Y. and Jasiuk, I. (1997) "Damage patterns and constitutive response of random matrix-inclusion composites", *Eng. Fracture Mech.* **58**, 581–606.

[19] Alzebdeh, K., Al-Ostaz, A., Jasuik, I. and Ostoja-Starzewski, M. (1998) "Fracture of random matrix-inclusion composites: scale effects and statistics", *Int. J. Solids Struct.* **35**, 2537–2566.

[20] Monette, L., Anderson, M.P., Ling, S. and Grest, G.S. (1992) "Effect of modulus and cohesive energy on critical fibre length in fibre-reinforced composites", *J. Mater. Sci.* **27**, 4393–4405.

[21] Termonia, Y. (1994) "Structure–property relationships in short-fibre-reinforced composites", *J. Polym. Sci.: Part B: Pol. Phys.* **32**, 969–979.

[22] Beale, P.D. and Duxbury, P.M. (1988) "Theory of dielectric breakdown in metal-loaded dielectrics", *Phys. Rev. B* **37**, 2785–2791.

[23] Kirkpatrick, S. (1971) "Classical transport in disordered media: scaling and effective-medium theories", *Phys. Rev. Lett.* **27**, 1722–1725.

[24] Torquato, S., Hyun, S. and Donev, A. (2002) "Multifunctional composites: optimizing microstructures for simultaneous transport of heat and electricity", *Phys. Rev. Lett.* **89**, 266601–266604.

[25] Cahn, J.W. and Hilliard, J.E. (1958) "Free energy of a nonuniform system. I. Interfacial free energy", *J. Chem. Phys.* **28**, 258–267.

[26] Cahn, J.W. (1965) *J. Chem. Phys.* **42**, 93.

[27] Oono, Y. and Puri, S. (1987) "Computationally efficient modeling of ordering of quenched phases", *Phys. Rev. Lett.* **58**, 836–839.

[28] Oono, Y. and Puri, S. (1988) "Study of phase-separating dynamics by use of cell dynamical systems. I. Modeling", *Phys. Rev. A* **38**, 434–453.

[29] Chen, K. and Ma, Y-Q. (2002) "Ordering stripe structures of nanoscale rods in diblock copolymer scaffolds", *J. Chem. Phys.* **116**, 7783–7786.